

The Development and Numerical Modeling of a Chua Circuit as a Pedagogical Tool

Trent Ziemer

The Physics Department at the College of Wooster, Wooster, OH, 44691, USA

(Dated: December 10, 2014)

The electrical circuit created by and named for Leon Chua was constructed using discrete components and then compared with two computational models. The goal was to provide a hardware and software package to demonstrate the link between basic circuits and both non-linear dynamics and the construction of more complicated electronics. The physical circuit was made from resistors, capacitors, and operational amplifiers, and an oscilloscope was used to compare the circuit's state with the numerical model. The model was implemented in a program written in C and a user interface was created using AutoHotkey. The program output was then compared with experimental data from the circuit and the accepted data to confirm the accuracy of each. The circuit was finally reconstructed to be more compact and user-friendly, while the program was updated and finalized to provide a comprehensive tool to students.

Contents

I. Introduction	1
II. Overview of the Chua Circuit	2
III. Physical Theory	4
IV. Numerical Computation	5
V. Procedure	6
VI. Results and Conclusions	7
VII. Future Work	9
VIII. Acknowledgments	9
References	9

I. INTRODUCTION

The availability of resources concerning low-level electronics is varied and widespread through many mediums. There is almost always a way to find help with any type of problem or particular circuit, from Horowitz and Hill to the IEEE journals, from Internet hobbyist guides using breadboards to professionally made printed boards, from Ohm's law to digital signal processing. In addition, studies of chaotic dynamics, such as bifurcation diagrams and fractals, are widely discussed and mathematically standardized within the communities of physics, mathematics, and electronic engineering. Despite the extent of study on the intersection of these two fields, comprehensive resources introducing the material are surprisingly lacking. The Chua circuit is one of the most commonly studied systems in non-linear dynamics, yet there are few resources that even attempt to cover all aspects of the system. Those that do are too focused on the perspective of their own fields to be understood by those

from other fields. The lack of information on non-linear dynamics in electronic circuits, especially the Chua circuit, has created the demand for interdisciplinary and comprehensive resources that demonstrate the principles of electronic design and computer modeling to introduce this paradigmatic circuit.

The theory of chaotic systems arose around 1900 from the work of Henri Poincaré, Jacques Hadamard, Andrey Kolmogorov, and others. The study of these systems, and many others, has been in a golden age since the 1960s due to the use of computers. The pioneers of electrical chaos in particular include Edward Lorenz, whose atmospheric equations resemble the equations for the Chua circuit and were instrumental in motivating later theorists; Mitchell Feigenbaum, who has studied bifurcations in the long-term values of the logistic map; and Leon Chua, who has created and done extensive work on what is commonly called "Chua's circuit"¹, the subject of our study.

The use of computers has made the study of atmospheric behavior, economics and econometrics, and electrical systems much more efficient and, in some cases, possible at all. For example, studies of the Lorenz equations revealed the "butterfly attractor" for certain parameter values, pictured in Fig. 1, while studies of the logistic map have revealed interesting bifurcations (doubling in the possible long term values of a function), as shown in Fig. 2. These distinct geometric objects are prime subjects of study in fields like mathematical topology and non-linear dynamics. Attractors, in particular, are interesting because they reveal the long-term behavior of a system; if a system of equations has an attractor, then, given certain conditions, the state of the system will always end up on the given attractor, though it is difficult to predict exactly where.

In the Chua circuit, the most famous chaotic geometric

[1] This refers to the general circuit that is studied. We will be discussing our implementation of Chua's circuit, and so it will be referred to in this paper as the 'Chua circuit'.

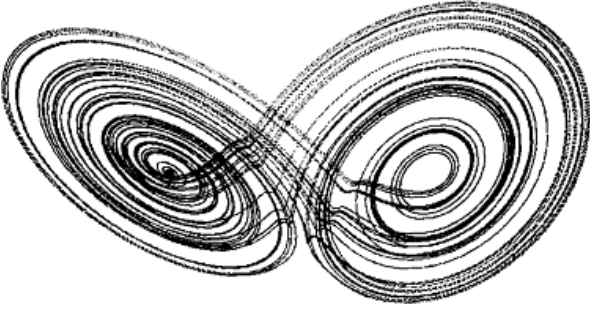


FIG. 1: A plot of the “butterfly” Lorenz attractor [1].

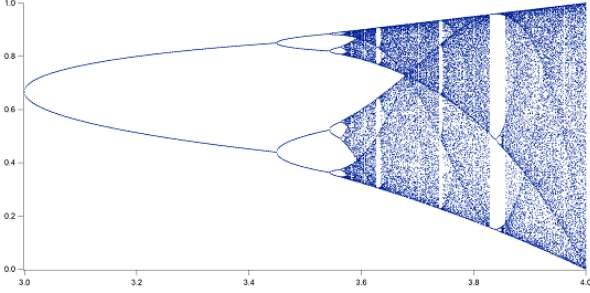


FIG. 2: A plot of the logistic map, enlarged to the region of $r = 3$ to $r = 4$.

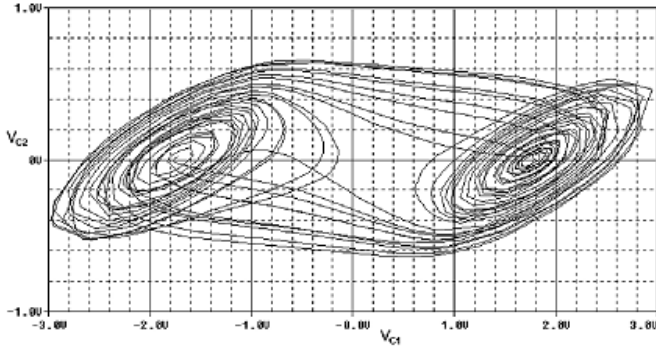


FIG. 3: A plot of a simulated double scroll attractor in the Chua circuit provided by Kilic [7].

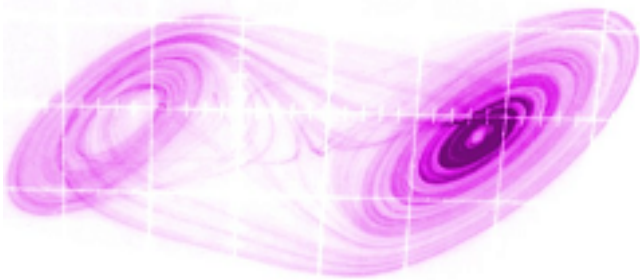


FIG. 4: A oscilloscope plot of a double scroll attractor in a physical Chua circuit provided by Siderskiy [9]. Image color has been inverted to show detail.

object is the double scroll attractor, which can be seen, as produced by a computational and physical model, respectively, in Figs 3 & 4. The Chua circuit has emerged as one of the most prominent examples of a chaotic system because it displays incredibly versatile behavior, but is still relatively simple [8]. This makes it a perfect system to study for those trying to become more familiar with each of the related fields.

II. OVERVIEW OF THE CHUA CIRCUIT

The Chua circuit is an autonomous non-linear electronic circuit made from discrete components that exhibits a wide range of behaviors associated with chaos. The state of the circuit at any given time is governed by three ordinary autonomous linear differential equations, each concerning the time derivative of a voltage or current in the circuit. Physically, the three variables are the voltage across either capacitor, and the current through the inductor to ground. The exact equations for these dynamics are included in Fig. 5, which is in the form derived electronically, and in Fig. 6, which has been converted to a mathematically-minded form. This form is also used in the code of the numerical model because it is more simple to follow. The greek-letter parameters in Fig. 5 are proportional to the physical resistances and capacitances of the circuit as in Fig. 6.

$$\frac{dV_{C_2}(t)}{dt} = \left(\frac{1}{R_9 C_2} \right) (V_{C_1}(t) - V_{C_2}(t)) - \left(\frac{1}{C_2} \right) f(V_{C_2}(t)) \quad (8)$$

$$\frac{dV_{C_1}(t)}{dt} = \left(\frac{1}{R_9 C_1} \right) (V_{C_1}(t) - V_{C_2}(t)) + \left(\frac{1}{C_1} \right) I_L(t) \quad (9)$$

$$\frac{dI_L(t)}{dt} = \left(\frac{1}{L} \right) V_{C_1}(t) - \left(\frac{R_{\text{internal}}}{L} \right) I_L(t) \quad (10)$$

FIG. 5: The system of differential equations describing the behavior of the Chua circuit in terms of time-dependent physical variables.

$$\begin{aligned} \frac{dV_{C_2}}{dt} &= \alpha[V_{C_2}(t) - V_{C_1}(t)] - \eta[f(V_{C_2}(t))] \\ \frac{dV_{C_1}}{dt} &= \beta[V_{C_2}(t) + I(t)] - \xi[V_{C_1}(t)] \\ \frac{dI}{dt} &= \gamma[V_{C_1}(t)] - \rho\gamma[I(t)] \end{aligned}$$

FIG. 6: The system of differential equations describing the behavior of the Chua circuit in terms of time-dependent variables.

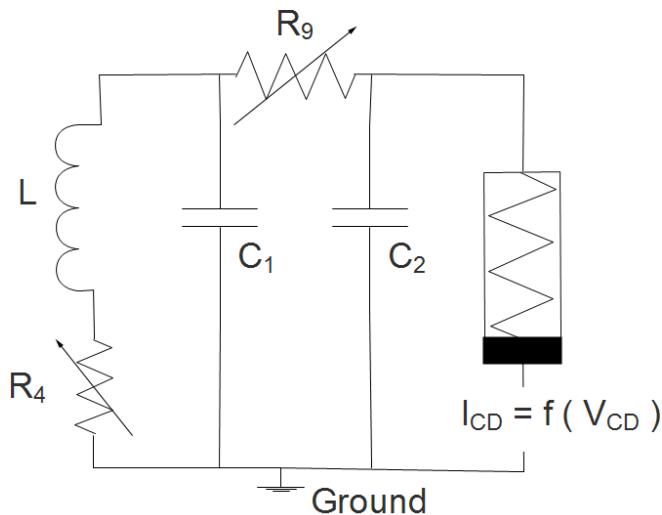


FIG. 7: A circuit diagram of the Chua circuit in its most common form. Notice that there are no clearly-defined inputs; however, there is a ground plane into which most elements have their ‘negative’ terminal.

The essential circuit diagram for the Chua system is shown in Fig. 7; however, a more complicated selection of components must be used to realize the circuit. This diagram is functional, but does not show the sub-components that comprise the inductor and Chua diode, which are not available as discrete components themselves and must be synthesized in the lab. The inductor must be made from other discrete components (resistors, capacitors, and transistors) because real inductors have too high of an internal resistance for our purpose. The Chua diode is more complicated, but can be made in several distinct ways. The final stage, the capacitor-resistor-capacitor (CRC) stage, is made from common electronic components.

Because the Chua diode, seen on the right side of Fig. 6, is non-linear, the circuit will function in a non-linear way. This means that the output is not necessarily proportional to the input. Although formally there are no inputs or outputs to the circuit other than the power supply voltages, any variable in the circuit’s system of state equations could be considered an output. The Chua diode is a peculiar component because it cannot be made from a single component nor does it function as a diode. Reasons for calling it the Chua diode are purely historical [11]. It actually operates as a non-linear negative resistor. This means that it works in a circuit the exact opposite way that a normal positive resistor does. A positive resistor drops a voltage across its terminals proportional to the current through it; a negative resistor adds a voltage to the circuit across its terminals proportional to the current through it.

The exact implementation used to create the Chua diode is unimportant as long as its resistance is non-linear and negative at ‘most points’ along the $i-v$ characteristic of the device. The $i-v$ characteristic is the relationship

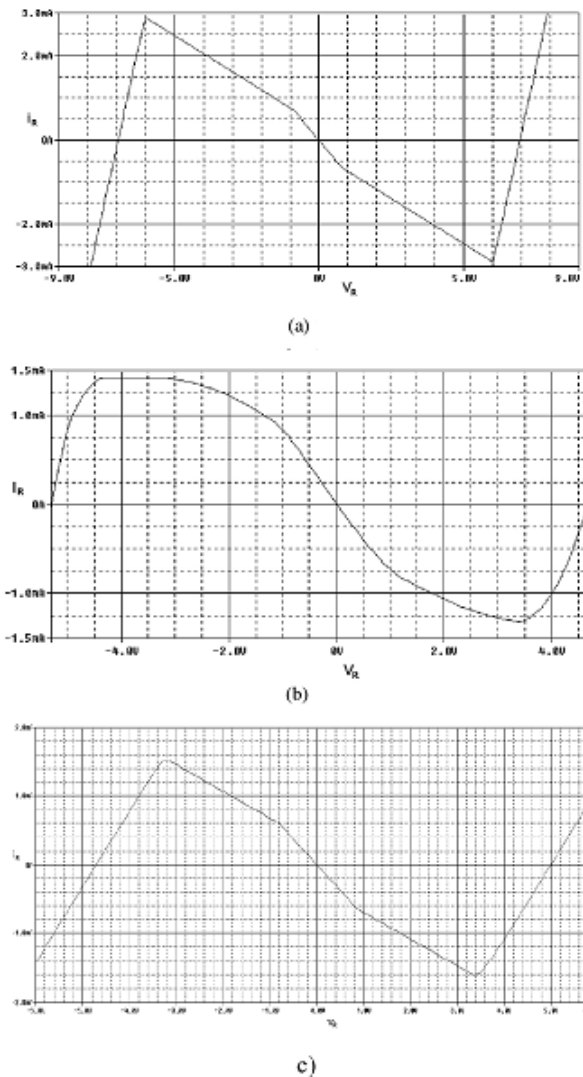


FIG. 8: a) An example $i-v$ characteristic of Chua diode made using parallel negative impedance converters, producing a piecewise-linear curve. b) An example $i-v$ characteristic using parallel operational transconductance amplifiers, producing a very rounded curve. c) An example $i-v$ characteristic using two parallel specialized op-amps called nullors, producing a slightly rounded piecewise-linear curve. [7]

between current and voltage through and across the device, usually plotted to give an idea of the operation of semiconductor devices like diodes and transistors, and has a slope equal to the admittance, or the inverse of the resistance.

Many different types of $i-v$ characteristics can be used to produce the Chua circuit; however, the simplest implementation is the kinked line as shown in Fig. 7a. This variant of the Chua circuit contains two parallel negative impedance converters (NICs) to make up the Chua diode. It can be divided into two proportional components that have a clear contribution to the overall characteristics of

the Chua diode, and even then the negative impedance converters are not too overwhelming for a novice user who would like to investigate the finer details of the system. Two other possible $i-v$ characteristics are shown in Fig. 7b and 7c. All known implementations of Chua diodes have a second kink in the direction of a positive resistor at larger absolute voltages, due to op amp breakdown effect. Fortunately, these voltages are never reached in typical Chua circuits.

III. PHYSICAL THEORY

Linear circuits are relatively simple. The operation of any number and combination of capacitors, resistors, and inductors can be learned in a first semester electronics class, and can be modeled and understood through basic physical theory. Even though the mathematics of differential equations and the abstract nature of a negative resistor can be difficult to comprehend, the Chua circuit can still be understood through the deceptively simple physical laws that govern circuits. Kirchhoff's circuit laws for current and voltage are expressed in a condensed form in Fig. 9, and are the most common way to apply Maxwell's equations to solve linear circuit problems.

The circuit can be analyzed using Kirchhoff's laws to produce equations for the current through the inductor and the voltage across each of the capacitors, as shown in the full diagram of the Chua circuit in Fig. 10. Note that resistors R_4 and R_9 are implemented as two variable resistors in series. One is a rough preset so that the other, with a finer tuning, can be adjusted to more easily look at the development of chaotic objects, which can appear then disappear with a change of a few ohms.

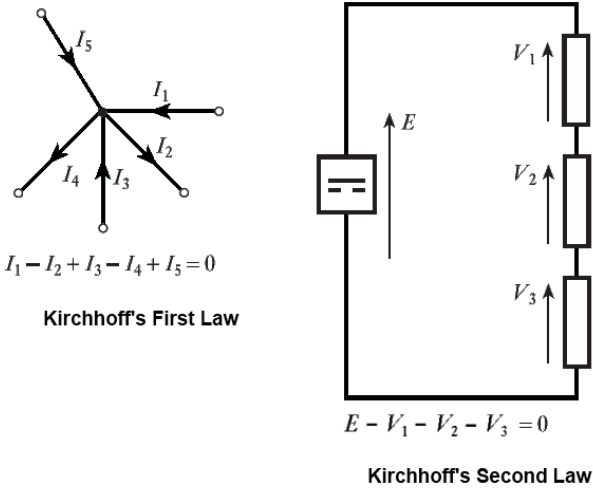


FIG. 9: Two diagrams of Kirchhoff's current and voltage laws, which are instrumental in analyzing any analog electronic circuit.

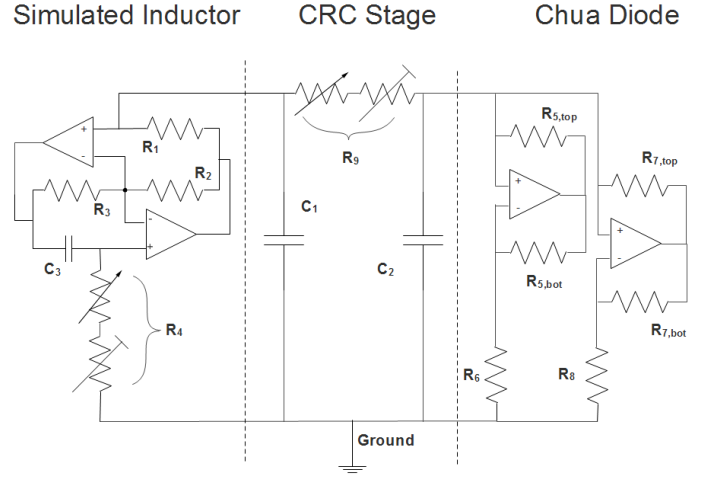


FIG. 10: The standard circuit diagram for this implementation of the Chua circuit.

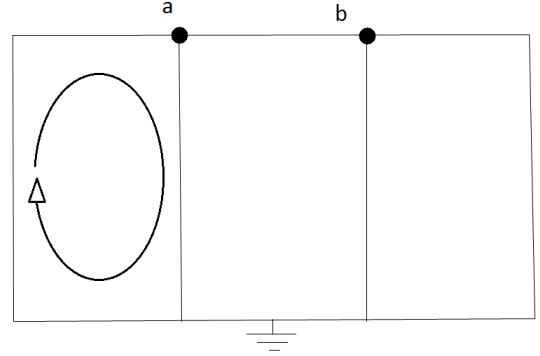


FIG. 11: The Chua circuit without components or labels to show the application of Kirchhoff's laws. The equations of the circuit are derived by examining the voltage ring, including the inductor and first capacitor, and the currents into and out of the nodes a and b .

Analyzing the voltage drops and gains around the loop as indicated in Fig. 11, it is determined that

$$V_L = V_{inductor} + V_{internal} = L \frac{dI_L}{dt} + V_{internal} = V_{C1} \quad (1)$$

where V_L is the voltage drop across the real inductor L , which includes the ideal simulated inductor and an internal resistance (with voltage drop $V_{internal}$). The equations for this resistance, in terms of I_L is

$$V_{internal} = I_L R_L, \quad (2)$$

where R_L is defined to be the internal resistance of the real inductor. Rearranging Eqn. 1 with this new knowledge yields the first equation governing the Chua circuit,

$$\frac{dI_L}{dt} = \frac{1}{L}V_{C_1} - \frac{R_{internal}}{L}I_L, \quad (3)$$

where the time derivative of the current through the inductor at any time is proportional to the difference between the voltage across the first capacitor and the current through the inductor at that time.

Analyzing the currents through point a yields that

$$C_1 \frac{dV_{C_1}}{dt} = I_L + \frac{(V_{C_1} - V_{C_2})}{R_9}, \quad (4)$$

where the current through C_1 goes from ground to a , then splits into a current going down through the inductor and over through R_9 , which has a voltage drop equal to the difference between the voltage across the capacitors to ground. This relationship can be rearranged to yield the second equation that governs the Chua circuit,

$$\frac{dV_{C_1}}{dt} = \frac{1}{C_1}I_L + \frac{1}{C_1R_9}V_{C_1} - \frac{1}{C_1R_9}V_{C_2}. \quad (5)$$

Finally, the current going from point a to point b splits into a current going through C_2 and a current applied to the Chua diode, which can be modeled mathematically as

$$\frac{(V_{C_1} - V_{C_2})}{R_9} = C_2 \frac{dV_{C_2}}{dt} + f(V_{CD}), \quad (6)$$

where the function of V_{CD} is the $i-v$ characteristic. Simplifying this relationship, and realizing that the voltage across the second capacitor and Chua diode must be the same, yields

$$\frac{dV_{C_2}}{dt} = \frac{1}{R_9C_2}V_{C_1} - \frac{1}{R_9C_2}V_{C_2} - \frac{1}{C_2}f(V_{C_2}), \quad (7)$$

the final equation governing the operation of the Chua circuit in our implementation. Note that the current directions and capacitor labels differ in this paper from some other sources, and should not be confused [1, 3, 12]. Functional dependence on time has been excluded where applicable. Voltages and currents are the only variables that change with time; capacitances and resistances do not.

The terms from Eqns. 3, 5, & 7 can then be rearranged and formulated into the equations from Figs. 5 & 6 as expected. Even with the knowledge that the equations as they were shown previously are a good description of the behavior of the circuit, it is still difficult to determine the exact voltages or currents at any given time. One must confirm the physical circuit with a theoretical model that is usually implemented computationally.

IV. NUMERICAL COMPUTATION

Modeling of physical systems is often done with computers because the systems frequently become more complicated to model as the system itself increases in detail or complexity. Numerical computational methods are often employed with differential equations that are not solvable with analytical methods, or when dealing with certain systems that would take too long to solve without the aid of computers. The monolithic Runge-Kutta methods are one of the most common ways to numerically solve a system of ordinary differential equations.

The specific procedure used to compute successive values of each variable matters significantly less than simply using the method correctly. While this implementation uses the widely-known Runge-Kutta 4 method because it is a good midpoint between the simple Euler's methods and the more advanced methods like the modified Runge-Kutta-Fehlberg 45, almost any valid differential equation modeling method could be used.

The first method, abbreviated RK 4, and the slightly error-corrected Runge-Kutta-Fehlberg method, which is abbreviated RKF 45 ("four-five"), are both more accurate than the classical Euler method. The circuit will be modeled with an RK 4 method in a C program that will be compiled, along with the user interface, into an executable file. The general algorithm for the RK4 method as used in our system of equations is seen in the flowchart in Fig. 12. An explanation of the mechanics of the Runge-Kutta 4 method is outside the scope of this paper; however, it can be summarized as a quick and reliable way to track the state of the Chua system so long as step size and parameter values are small compared to the length of time computed.

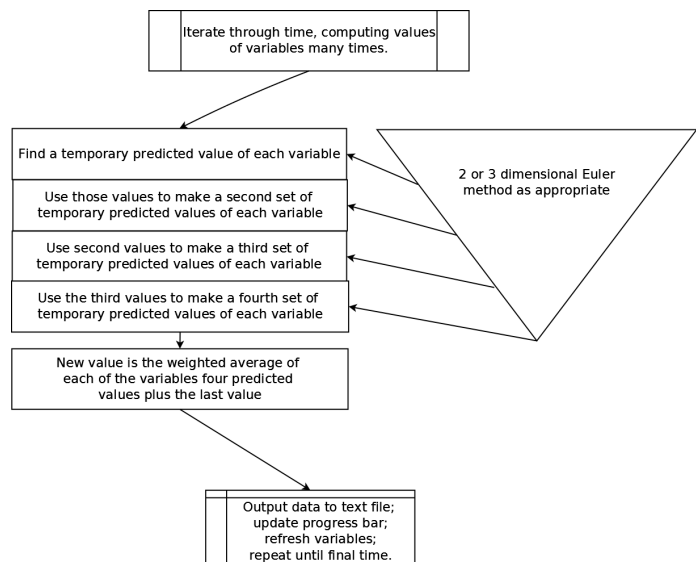


FIG. 12: A flowchart demonstrating how the Runge-Kutta method was used to solve the initial value problem describing the Chua circuit given the four initial conditions.

Several bridges between different parts of the program must be made before, after, and during the execution of the RK 4 so that it can function properly in the context of the users instructions. Thus the algorithm is implemented in a C language program (compiled into an executable file) that declares variables, reads parameters from a plain text file, runs the RK4 method, and iterates through time, outputting the data to a different plain text file. The front end governs the operation of the back end for the user and is implemented in the Auto-Hotkey scripting programming language. The AHK program serves as a graphical interface for the user to input parameters and initial conditions and then prompts the user to open the text file to view the data. The overall algorithm of the software program, including the front end user interface and back end RK 4 computational method, is included in Fig. 13.

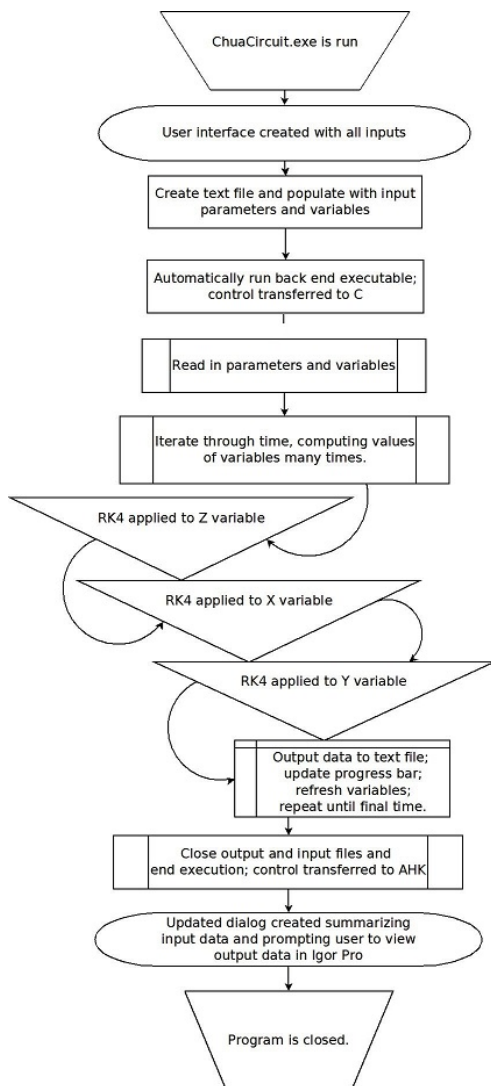


FIG. 13: An overview of the software algorithm for creating a data set from given inputs. Steps in boxes with rounded edges are visible to the user, while triangles indicate a sequence containing many smaller steps.

Using the initial values of each of the variables, the computational version of the parameters, and the equations of the Chua circuit contained in Fig. 6, the algorithm estimates the next three values and continues doing so until the final time, recycling the last three values of each variable to compute each variable at the next step. It periodically outputs these values to a plain text file. Usually only every 1000th or so value is actually recorded in the file to reduce the amount of data that needs to be processed by the graphical utility; however, intermediate values must still be computed to maintain accuracy.

V. PROCEDURE

The two major parts of the project were developed independently and then mutually incorporated to verify the results of each.

First, the software package was created using a combination of the C and AHK languages to produce a single folder containing, among other necessary files, an executable program to take variable input from the user and output data into a text file as specified previously.

Second, the physical circuit was created using discrete electronic components and tested with relevant accessories. The CRC stage and power supply switch, the simulated inductor, and Chua diode were each constructed on separate breadboards so that they could be individually tested and so that the correct operation of the preliminary circuit could be verified. Fig. 14 shows the collection of all three stages of the circuit alongside measurement tools and the power supply at this first stage of construction.

After the circuit was completed, the three variables were plotted parametrically against each other with respect to time on an oscilloscope and several double scroll attractors were observed. This confirmed that the Chua circuit was operating correctly. The next goal was to refine the circuit for ease-of-use by the next user and clarity.

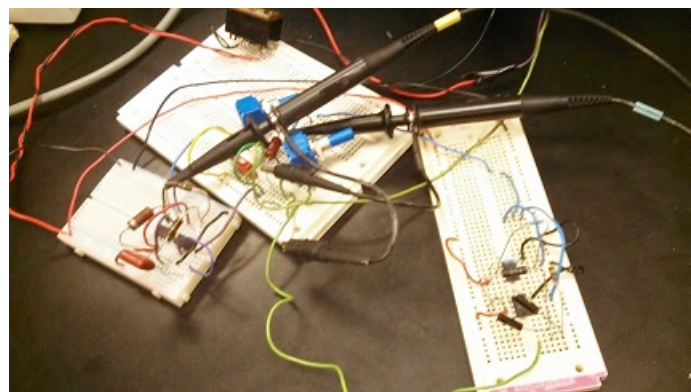


FIG. 14: Pictures of the inductor, CRC stage and power switch, and Chua diode being integrated to form a prototype of the Chua circuit.

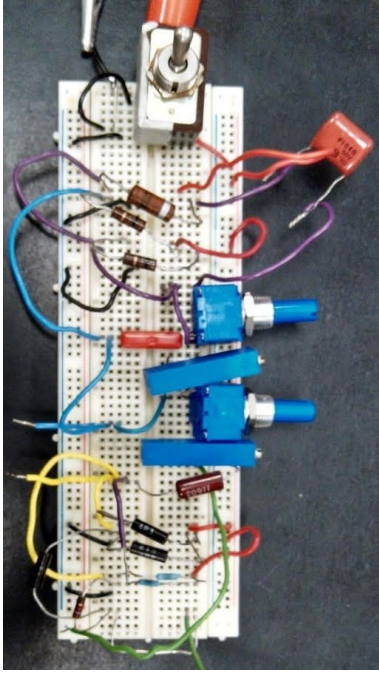


FIG. 15: A picture of the integrated Chua circuit on a single breadboard. Measurement of the voltages is made on the left side with the blue and yellow wires; the ground is at the bottom; power supply wires and switch are at the top.

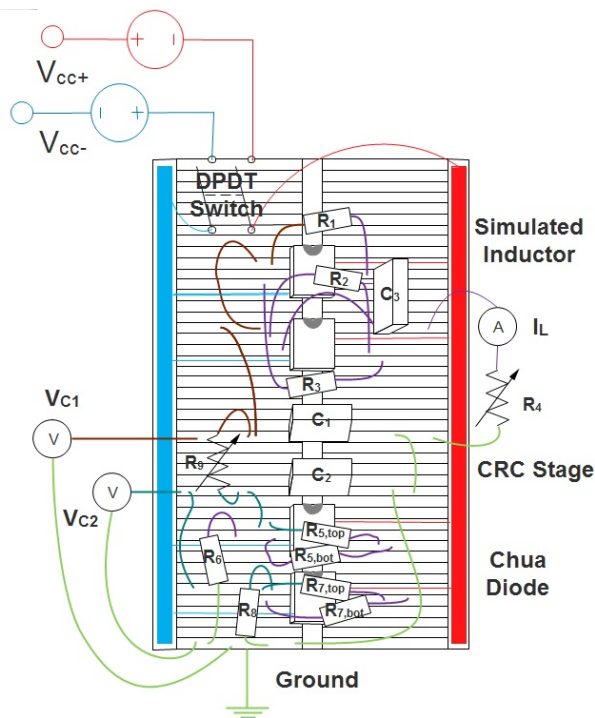


FIG. 16: A pin-level diagram of the Chua circuit. This is an electronic circuit diagram where the pin connections and physical locations of components are shown to compromise between a traditional diagram and a picture of the circuit itself.

Component	Value	Unit	Max.
R_1	99	Ω	
R_2	103.2	Ω	
R_3	1000	Ω	
R_4	1360	Ω	2500
$R_{5,top}$	17.63	k Ω	
$R_{5,bot}$	17.74	k Ω	
R_6	2706	Ω	
$R_{7,top}$	212.8	Ω	
$R_{7,bot}$	213.3	Ω	
R_8	1442	Ω	
R_9	260	Ω	2500
C_1	102	nF	
C_2	9.2	nF	
C_3	99.2	nF	
L	119	mH	
U_1	-0.3719	mS	
U_2	-0.6951	mS	
G_a	-0.704	mS	
G_b	-0.372	mS	
V_{cc+}	15	V	
V_{cc-}	-15	V	

TABLE I: A table of experimental component values used in the circuit. The Max. column indicates the range of the variable resistors.

The circuit was then transferred to a single breadboard with a superior layout and more logical organization as in Fig. 15. The potentiometers were oriented on the edge of the board so that they could be easily adjusted, and leads to the power supply and important points in the circuit were added so that users could easily interface with the circuit and troubleshoot components. These points include ground and a lead to the ends of either capacitor. A circuit diagram of the physical layout of the final circuit is included in Fig. 16. Each different color of wire in the diagram represents a voltage equipotential, except purple. Table I contains the parameter values used in the experimental circuit.

VI. RESULTS AND CONCLUSIONS

The physical Chua circuit was successfully constructed and demonstrated the ubiquitous double scroll attractor. In Figs. 17 & 18 on the next page are parametric oscilloscope plots of the double scroll attractor for two slightly different parameter values, as indicated in Table II. Another similar image was also produced, as seen in Fig. 19. The vertical axis is V_{C_2} , while the horizontal axis is V_{C_1} . A distortion of the same double scroll attractor can be observed for any resistances within about 20Ω of either parameter.

#	Plot	R_4 (Ω)	R_9 (Ω)
1	Fig. 26	255	1355
2	Fig. 27	265	1365
3	Fig. 28	595	1710

TABLE II: A table of parameter values that produced double scroll attractors in plots of V_{C_2} versus V_{C_1} .

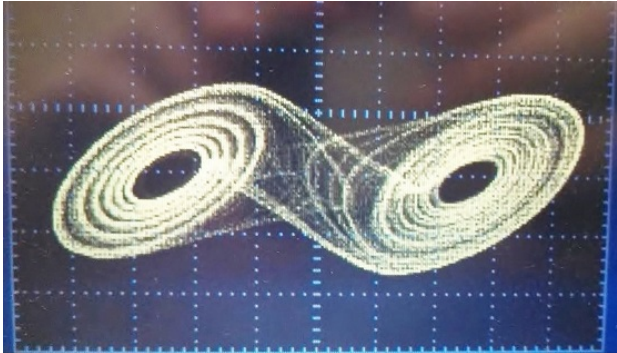


FIG. 17: A picture of the first attractor produced by the experimental Chua circuit. Experimental parameter values are $R_4 = 255 \Omega$ and $R_9 = 1355 \Omega$.

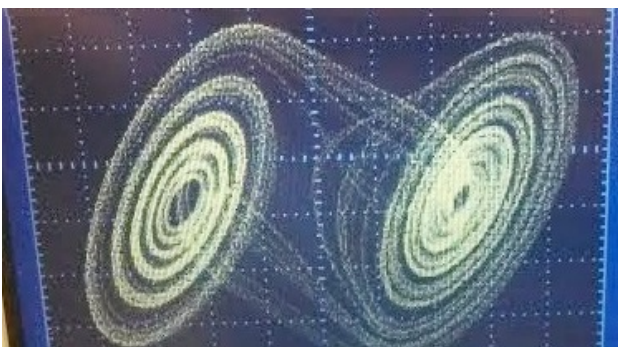


FIG. 18: A picture of the second attractor produced by the experimental Chua circuit. Experimental parameter values are $R_4 = 265 \Omega$ and $R_9 = 1365 \Omega$.

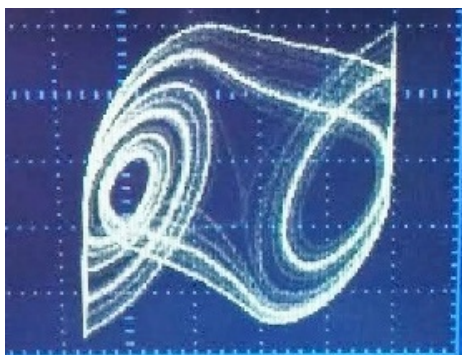


FIG. 19: A picture of the third attractor produced on the experimental Chua circuit. Experimental parameter values are $R_4 = 595 \Omega$ and $R_9 = 1710 \Omega$.

Unfortunately, these are the only data plots available. After transferring the circuit to the single breadboard in order to make a more compact circuit, the circuit stopped working, and no more data could be produced. While the exact nature of the malfunction is unknown, it was probably related to the op amps in the circuit. Each component was removed from the circuit and analyzed for any defects; however, the only fault seemed to be in the op amps. A wide array of op amps were tested several times each in non-inverting and inverting amplifiers, but still did not operate as expected. No further conclusions could be made about the physical circuit or its relation to other models because of this malfunction.

The program can successfully be used to demonstrate both chaos and a wide variety of chaotic behavior but is currently unable to corroborate with the limited physical data produced, due to the malfunction of the circuit mentioned previously. A sample plot of a different attractor by Siderskiy [9] can be plotted alongside the matching computational plot from the program to confirm that it matches previous theory. There is a strong correlation between each attractor as shown in Figs. 20 and 21.

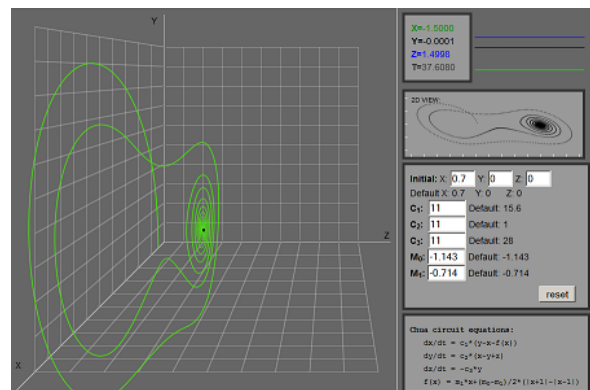


FIG. 20: A picture of Siderskiy's simulation [9] showing the beginning of an attractor, with all equation parameters (except the Chua diode slope) equal to 11. In particular, note the 2-d plot on the top right which closely matches our plot in Fig. 21.

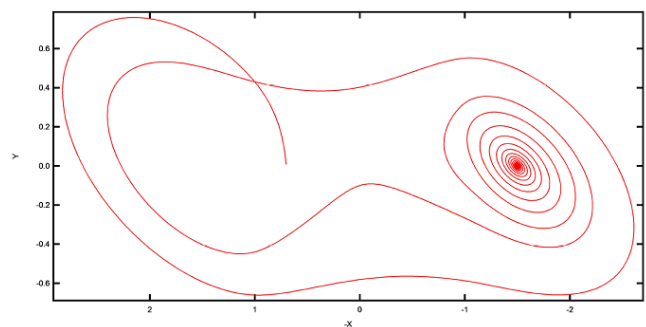


FIG. 21: A plot of my simulation's output with inputs matching those from Siderskiy's [7] in Fig. 20. The shape is more important than the particular values or variables.

VII. FUTURE WORK

One of the most promising aspects of this experiment is that, because it is a first step into a new development, there is a plethora of avenues in which more work can be done. In every aspect of this endeavor, improvement is needed or more detail desirable. Beyond getting the physical circuit to work again, there is important work to be done.

The software package, in particular, probably has the most room to grow. Though AHK is a useful tool for small-scale programs, combining CSS with JavaScript would be a much better platform to create a package that is clean and appealing to all users. Another area would be customizeability: parameters, equations, and methods. It would be best if the user had a wide variety of choices for each of these, especially if there were built-in tools for visualization in parameter space and in the context of the circuit. Because our project focuses on bridging the gap between electronics and the mathematical model, emphasizing the relationship between the two is critical. The program currently produces a diverging output in all three dependent variables for some initial conditions and parameter values. Though a wide range of parameter space is available for useful computation, a significant amount of theoretical and practical work could be done to find the causes of these divergences and remedy this rather large issue

Even with the initial creation of this prototype, much work can still be done to make it a feasible product. All

suggestions mentioned so far involve direct human labor, while manufactured boards and housings would be most appropriate for cost and time reasons. Even more desirable would be to make this particular Chua design on an integrated circuit chip. Because the inductor is simulated, it would only be a matter of engineering to design a 16-pin integrated circuit. Currently, a working Chua circuit on a simple breadboard with discrete components would cost about \$28 in components and roughly two hours in labor time, assuming good electronic lab equipment is already available. Realistically, it would cost an immense amount to gather the equipment, machinery, and skilled personnel to begin producing Chua circuits to meet even the small demand expected from universities and development teams.

VIII. ACKNOWLEDGMENTS

I would like to thank Dr. Lehman for her assistance and guidance with the electrical circuit throughout the project. I would like to thank Joey Smith for discussing programming with me and editing my model. Dr. Pasteur of the Mathematics department, as well, assisted me with creating a working numerical model. I also appreciate the extensive feedback of my chief editor Samantha Shoemaker. Finally, this project would not have been possible without funding and the necessary tools, technology, and devoted academic atmosphere from the Department of Physics at The College of Wooster.

-
- [1] R. Brown. *Generalizations of the Chua Equations*. IEEE Transactions on Circuits and Systems, 1993, 40, 11, 878-884.
 - [2] C. Mallett and J. Bennett. *AHK Help Online File*. 2014.
 - [3] L. Fortuna. *Chua's Circuit Implementations: Yesterday, Today and Tomorrow*. World Scientific Publishing Company, Singapore, 2009.
 - [4] C. P. Hong. *Computer Modeling of Heat and Fluid Flow in Materials Processing*. IOP Publishing, United Kingdom, 2004.
 - [5] P. Horowitz and W. Hill. *Art of Electronics*. Cambridge University Press, United Kingdom, 1989.
 - [6] J. Sprott and Z. Elhadj. *The Discrete Hyperchaotic Double Scroll*. World Scientific Publishing Company, 2009, 19, 3, 1023-1027.
 - [7] R. Kilic. *A Practical Guide for Studying Chua's Circuits*. World Scientific Publishing Company, Singapore, 2010.
 - [8] C. Letellier and R. Gilmore. *Topology and Dynamics of Chaos: In Celebration of Robert Gilmore's 70th Birthday*. World Scientific Publishing Company, Singapore, 2013.
 - [9] V. Siderskiy. *Chua's Circuit Simulator*. 2014, <http://www.chuacircuits.com/sim.ph>.
 - [10] T. Lovett, A. Monti, F. Ponci. *Automatic synthesis of uncertain models for linear circuit simulation: A polynomial chaos theory approach*. Elsevier Science, 2008.
 - [11] K. Thamilmaran and M. Lakshmanan. *Classifications of Bifurcations and Routes to Chaos in a Variant of Murali-Lakshmanan-Chua Circuit*. International Journal of Bifurcation and Chaos, 2001, 12, 783-813.
 - [12] T. Ueta. *Chaos in Circuits and Systems*. World Scientific Publishing Company, Singapore, 2002.